REPORT DOCUMENTATION PAGE

Form Approved
OMB No. 0704-0188

1. AGENCY USE ONLY (Leave blank)	2. REPORT DATE	3. REPORT TYPE AND DATES COVERED
	August 1996	Technical (interim)

4. TITLE AND SUBTITLE
Atmospheric corrections for mid-IR (3-5 micrometer) spectroscopy

5. FUNDING NUMBERS
C#N00014-91-C-0028
G#N00014-94-1-0421

6. AUTHOR(S)
Karl W. Bornhoeft
Paul G. Lucey
Keith A. Horton

7. PERFORMING ORGANIZATION NAME(S) AND ADDRESS(ES)
Hawaii Institute of Geophysics & Planetology
University of Hawaii
2525 Correa Rd.
Honolulu, HI 96822

8. PERFORMING ORGANIZATION REPORT NUMBER
2818-02

9. SPONSORING/MONITORING AGENCY NAME(S) AND ADDRESS(ES)
Office of Naval Research
Headquarters
800 N. Quincy
Arlington, VA 22217

11. SUPPLEMENTARY NOTES
Scientific paper to be published in proceedings in conjunction with August 1996 International Society for Optical Engineering (SPIE) conference in Denver, CO, on terrestrial remote sensing.

12a. DISTRIBUTION/AVAILABILITY STATEMENT
distribution unlimited

12b. DISTRIBUTION CODE

13. ABSTRACT *(Maximum 200 words)*

Terrestrial spectroscopy in the 3-5 micrometer wavelength region offers unique applications, such as detection of carbon and sulfur compounds, and temperature determination of ground fires and volcanic lava flows. We collected airborne hyperspectral images with a Fourier transform spectrometer over seawater in a tropical environment combined with radiosonde data and MODTRAN atmospheric modeling. We applied the results from these data to spectra collected of the same locations at different times without supporting radiosonde data, to assess surface radiance accuracy and atmospheric variability. This resulted in remotely-sensed ground temperature accuracies averaging ±5 Kelvin, comparable to space-based AVHRR single-channel accuracies.

14. SUBJECT TERMS
infrared, spectroscopy, atmospheric, Fourier, MODTRAN

15. NUMBER OF PAGES
10

16. PRICE CODE
N/A

17. SECURITY CLASSIFICATION OF REPORT	18. SECURITY CLASSIFICATION OF THIS PAGE	19. SECURITY CLASSIFICATION OF ABSTRACT	20. LIMITATION OF ABSTRACT
UNCLASSIFIED	UNCLASSIFIED	UNCLASSIFIED	UL

Atmospheric corrections for mid-IR (3-5 micrometer) spectroscopy

Karl W. Bornhoeft, Paul G. Lucey, and Keith A. Horton

Hawaii Institute of Geophysics and Planetology
University of Hawaii at Manoa
Honolulu, HI 96822

ABSTRACT

Terrestrial spectroscopy in the 3-5 μm wavelength region offers unique applications, such as detection of carbon and sulfur compounds, and subpixel temperature determination of ground fires and volcanic lava flows. Two challenges in this region are the similar levels of solar reflected and terrestrial emitted fluxes, and the low values of both these fluxes making measurements of high quality more difficult than in the short-wave or long-wave IR regions. We collected airborne hyperspectral images with a Fourier transform spectrometer over seawater in a tropical environment combined with radiosonde data and MODTRAN atmospheric modeling, to distinguish ground radiances, atmospheric contributions, and spurious instrumental effects. Within the range of our radiosonde data (3 km altitude), MODTRAN very closely reproduces the sensor-detected mid-IR fluxes. Clear separation between solar reflected and terrestrial emitted components is achieved, and different atmospheric compositional spectral effects are analyzed. We applied the results from this well-truthed experiment, to spectra collected of the same locations at different times without supporting radiosonde data, to assess surface radiance accuracy and atmospheric variability.

keywords: infrared, spectroscopy, Fourier, atmospheric, MODTRAN

1. INTRODUCTION

The 3-5 μm wavelength region is a spectral range in the infrared not blocked by atmospheric absorptions (primarily from water vapor and carbon dioxide). This wavelength region has been used for determination of volcanic lava flow and ground fire temperatures, and detection of carbon, sulfur, phosphorous, and hydrocarbon compounds[15]. A unique challenge for utilization of the 3-5 μm band for remote sensing is the similar flux levels of solar reflected and terrestrial emitted radiance. Unlike the visible, near infrared and far infrared where only one or the other of these components contributes most of the flux, in the 3-5 μm band both components similarly contribute to the total energy flux received at a remote sensor . Also, the total radiance is low here, especially near 3 μm, making difficult both the detection and separation of these radiant sources (Figures 1 and 2). Meanwhile, as for any remotely sensed measurements of the Earth, the atmospheric transmittance and radiance must be accounted for to determine the true surface radiant flux for accurate surface temperatures and compositional information. We have combined spectra from the SMIFTS Fourier transform spectrometer, temperature data collected in-situ and from low-altitude radiosonde measurements, and the MODTRAN2 radiative transfer code. With these, we have analyzed data in the 3-5 μm wavelength region and applied it to surface temperature determination using two methods: the first method directly calculates an average surface brightness temperature from SMIFTS sensor-detected radiance corrected using MODTRAN2, and the second method iteratively uses MODTRAN2 with successive surface brightness temperature input values to model an at-sensor radiance that best fits the SMIFTS sensor-detected spectra. We describe the methodology, and results here.

2. SMIFTS INSTRUMENT AND DATA COLLECTION

We used a spatially modified imaging Fourier transform spectrometer (SMIFTS)[8]. Between 3-5 μm, it has a signal-to-noise ratio of 100-200, spectral resolution of 70 cm^{-1}, and an instantaneous field of view of 0.6 mrad. With SMIFTS, we have collected mid-wave infrared data over forest, desert, and tropical environments.

Our data consists of a series of spectral image cubes taken via helicopter approximately 2 km over the Natural Energy Laboratory/Hawaii Authority (NELHA) on the island of Hawaii. These data were collected throughout the daylight hours of May 14, 1994. NELHA is used for aquaculture and ocean thermal energy

conversion research, and includes the maintenance of open-air thermally-controlled seawater ponds. We used these ponds as calibration for the remotely-sensed helicopter-mounted SMIFTS collections, since water is spectrally "flat" in the 3-5 μm region[15]. Average 8-12 μm pond brightness temperatures were recorded by ground personnel, and near-ground air temperatures and relative humidities were also recorded. Furthermore, atmospheric radiosonde data from 0-3 km altitude of temperature, pressure, and relative humidity were collected for one of the pond overflights. Finally, Global Positioning System (GPS) location data for the helicopter's latitude and longitude were available throughout the day. With this well instrumented data set (which may be called "in-situ assisted remote sensing"), we could focus on determining the transmittance and radiance of the intervening atmosphere, to calculate true surface flux from the SMIFTS-detected radiance for surface temperature comparisons.

3. ATMOSPHERIC AFFECTS BETWEEN 3-5 μm

As described earlier, two main challenges for spectroscopy between 3-5 μm are the complexity of separating out the solar reflected and terrestrially emitted components, and the low total signal from both of these contributions, making acquisition of high quality data and scientifically useful interpretation difficult. A third concern, necessary to address in the accurate determination of ground radiances and spectral features from airborne and Earth-orbiting sensors in particular, is that of correcting for the affects of the atmosphere between the sensor platform and the ground target. The solution to the problem consists of characterization, correction, and removal of the affects of the intervening atmosphere on both emitted and reflected flux detected at the sensor.

Atmospheric affects have only begun to be quantitatively addressed in the 3-5 μm spectral region. In the visible to near-infrared, several authors have had good success. Blake and Singer[2] studied low-level atmospheric correction using water vapor density as a variable, and studies employing the Jet Propulsion Laboratory's Airborne visible/Infrared Imaging Spectrometer (AVIRIS) uses an extensive atmospheric modeling process[4,19]. In the thermal wavelength regions, however, there has been less comprehensive application of atmospheric corrections[5], and authors have had to make many simplifying assumptions which were mathematically convenient but did not yield accurate results.

The atmosphere both attenuates surface radiant flux and adds to the total radiant flux measured by a remote sensor. In the 3-5 μm spectral window, although the atmosphere is mostly transparent, there are localized major absorptions due to water vapor and carbon dioxide, as well as broad minor absorptions due to water vapor and a nitrogen continuum as well as carbon monoxide and methane, attenuating surface radiant energy reaching a sensor (Figure 3). Meanwhile, aerosols scatter solar reflected and terrestrial thermal energy as well as emitting to add radiant energy. In the 3-5 μm region for a moderate-resolution spectrometer at least 1 km in altitude, not only are the at-sensor solar reflected and terrestrial emitted fluxes similar, so are the sum of those two fluxes and the total atmospheric contribution (Figure 4). Especially in this spectral region of low absolute reflected and emitted solar terrestrial and relatively equal atmospheric radiances, it is necessary to account for both the atmospheric extinction and radiance.

Not part of the present focus but interesting to note, is that the process of removing atmospheric affects to determine correct ground radiances also yields useful information about the intervening atmosphere itself, such as details about its composition including water vapor and carbon dioxide, and state variables such as temperature and pressure. In this way, a "sounding" is taken for the atmosphere, as an indirect result of accounting for its affects on the ground target spectra.

4. MODTRAN ATMOSPHERIC MODELING

Our primary tool to model these atmospheric affects was MODTRAN2[1]. Radiosonde soundings were taken once, in the afternoon of the 14th, launched from about 7 km from NELHA. The radiosonde temperature and relative humidity as a function of altitude (which was calculated from pressure) up to 3 km were input to MODTRAN for atmospheric layer thicknesses of 0.2 km, and the MODTRAN tropical atmosphere model was used for higher altitudes. We used the MODTRAN multiple scattering option: although single scattering is sufficient for the most part in the mid-infrared, multiple scattering is important at high solar zenith angles[13] especially in the lower atmosphere[7], and its inclusion does not appreciably increase computer run time. The MODTRAN maritime

boundary layer (0-2 km), spring-summer (2-30 km), and background "stratospheric" (>30 km) aerosol models were used without modification: there are sulfate (SO_4^{2-}) aerosol compounds formed from SO_2 transported around the southern tip of Hawaii and up the western coast on a 160 km journey from degassing sources on Kilauea's summit and East Rift Zone[18], but these compounds have only broad or weak narrow absorption features between 3-5 μm overwhelmed by the water vapor and carbon dioxide features[14,17]. Even if non-aerosol SO_2 gas was dominant, our modeling shows that above-typical values[3] produce no measurable affects between 3-5 μm at 70 cm^{-1} spectral resolution. There was an occasional thin fog haze blowing but no rain or clouds on the 14th.

Since the radiosonde balloon was launched some distance from NELHA, and because the afternoon radiosonde data was to be applied at other times of the day, near-ground air temperatures and relative humidities were taken at NELHA concurrent with each helicopter overflight. The differences in temperature and relative humidity between these ground measurements and the surface-layer radiosonde values were added to several lower layers of the radiosonde inputs to MODTRAN, to allow for the radiosonde distance and time differences.

The seawater pond brightness temperatures were taken at NELHA with a Cyclops hand-held radiometer, concurrent with each helicopter overflight. For the afternoon (2:30 P.M.) data collection, which was concurrent also with the radiosonde launching, the at-surface brightness temperature value of one pond was input to MODTRAN. These parameters applied were applied to MODTRAN, convolved to the 70 cm^{-1} SMIFTS spectral resolution (MODTRAN2 highest spectral resolution is 2 cm^{-1}), and then compared to afternoon SMIFTS radiance taken of the same pond (Figure 5). For the most part the comparison of the model run to the measured radiance was very good, convincing us that the adjustments made to the lower atmospheric layers of the radiosonde inputs to MODTRAN were valid enough (at SMIFTS spectral resolution) to apply to NELHA pond overflights at the other collection times for surface temperature determination.

5. SURFACE TEMPERATURE DETERMINATION

The above-described MODTRAN final inputs, based on afternoon radiosonde data and known afternoon NELHA near-ground surface temperature and relative humidity, were applied to helicopter overflights with SMIFTS earlier on May 14th to assess the accuracy of surface radiance measurements using our atmospheric model corrections, primarily for surface temperature determination. The first step in this process was to decide how best to use the MODTRAN-modeled radiance. There are some purely atmospheric components to the modeled spectra which contain no information relating to surface radiance, such as the carbon dioxide feature near 4.3 μm and the encroachment towards 5 μm of a water absorption band near 6.7 μm. There are also some residual instrumental calibration artifacts in the measured spectra, especially near the increasingly low signal-to-noise towards 3 μm. We cannot adjust the model to account for the instrumental affects, but we can account for the atmospheric affects by excluding areas of the MODTRAN-modeled radiance where water vapor and carbon dioxide absorptions are strong. For this, we inspected the highest MODTRAN spectral resolution (2 cm^{-1}) transmittance (Figure 3) and excluded use of channels between 4.15-4.5 μm and longwards of 5.25 μm.

Using, then, regions of the spectra where transmittance is not dominated by atmospheric absorptions (Figure 6), we used SMIFTS spectra taken of two NELHA seawater ponds in the early daylight hours of the 14th (6:30 A.M.) and applied MODTRAN to determine their slightly different pond temperatures at that time. We chose two methods to do this, described and compared below.

The first method directly calculates an average surface brightness temperature from SMIFTS sensor-detected radiance corrected using MODTRAN2, using the following formula for at-sensor radiance:

$$L_t = (L_{bb} * \varepsilon_w * \tau_a) + L_a + L_g + L_s$$

where:

- L_t is the total SMIFTS-measured at-sensor radiance,
- L_{bb} is the blackbody emittance at the pond surface temperature(s) according to the Planck function,
- ε_w is the emissivity of the surface, assumed 0.975 for seawater[9,10,15]
- τ_a is the MODTRAN-modeled atmospheric transmittance between the surface

and the sensor,

L_a is the MODTRAN-modeled integrated atmospheric path radiance at-sensor,

L_g is the MODTRAN-modeled ground reflected radiance at-sensor, and

L_s is the MODTRAN-modeled path scattered radiance at-sensor.

The above formula was solved for L_{bb}. This provided calculated radiance values for 37 SMIFTS channels between 3.4 - 5.5 μm. We then calculated the brightness temperatures from each channel radiance value, excluding those channels where water vapor and carbon dioxide absorptions are strong. This provided us with 26 values of surface-equivalent temperature. From these we took an average. We did this for each of the two seawater ponds.

The second method iteratively uses MODTRAN2 with successive surface brightness temperature input values to model an at-sensor radiance that best fits the SMIFTS sensor-detected spectra. In other words, we did not use the above formula, but completed the full inverse of what we initially did to match MODTRAN to the afternoon SMIFTS measurements from the known afternoon pond temperature. We took the morning SMIFTS spectra, and ran MODTRAN several times at different surface temperatures, to find which MODTRAN case best matched the morning SMIFTS spectra. Two best-fit MODTRAN input surface temperatures were found, one for each pond, using the method of mean absolute deviation[12].

These methods of surface temperature calculation were also applied to a helicopter overflight of the same two ponds during late morning (11:04 A.M.). Results from the two methods for the two ponds at the two times are shown in the table below and in Figures 7 and 8. Also shown are the "actual" pond temperatures for each time (in Kelvin), as measured by ground personnel with the hand-held radiometer, as well as the root-mean-square deviation associated with each temperature.

Time	In-situ Radiometer Temperature	Method 1	Method 2
6:15 A.M.	296.3 ± 2.4	296.9 ± 2.7	297.5 ± 2.8
6:15 A.M.	299.7 ± 2.4	301.4 ± 5.1	301.5 ± 2.8
11:04 A.M.	297.3 ± 2.2	296.9 ± 6.9	294.2 ± 2.0
11:04 A.M.	301.3 ± 2.2	302.3 ± 7.7	297.7 ± 2.0

Of primary interest is that the temperatures determined using both methods are consistent with the radiometer-measured values, given the rms deviation associated with each value.

Of secondary interest is to note that method 1 gives the overall closest determined temperatures to the radiometer-measured values, even though method 2 gives the overall least root-mean-square deviation in each of those temperatures. These points follow from the nature of each calculation. Method 1 is calculated from the actual SMIFTS-detected radiance - which is more representative on average of true surface temperature even though it contains channel-specific instrumental and atmospheric "noise." Method 2 is calculated from MODTRAN-modeled radiance - which although it contains no "noise" and so produces a smoother radiance without spurious variation, is still modeled data and so is likely to be less accurate on average than measured data.

It is useful to compare the temperatures and rms deviations determined by each method to present capabilities of the NOAA Advanced Very High Resolution Radiometer (AVHRR) aboard the NOAA 9 satellite. That instrument is a standard yardstick for terrestrial surface temperature determination in the infrared. Kalluri and Dubayah[6] describe three methods of surface temperature calculation from AVHRR data, giving rms values between AVHRR and ground measurements of 2.01, 2.20, and 3.60 K, which are consistent with the generally accepted ±3 K absolute accuracy range for AVHRR. Higher accuracies have been obtained with AVHRR[11,16], but these have been

in tandem with data from other sensors and/or numeric algorithms which are not yet commonly accepted. Therefore, compared to standard AVHRR surface temperature rms accuracies, method 1 above ranges from at least as good to somewhat worse than AVHRR, while method 2 fares at least as good. It would be difficult to compare the absolute temperature determination accuracies of the above two methods to AVHRR without a more complete analysis of the accuracy of our hand-held radiometer and the instrumentation employed for the AVHRR ground truthing.

6. SUMMARY AND CONCLUSIONS

Recent advances in technological and computational capabilities, combined with the use of the most current version of radiative atmospheric modeling, is allowing useful spectroscopy in the 3-5 μm infrared region. This region was previously avoided due to low absolute levels of total radiation flux and the difficulty of separating the solar reflected and terrestrial emitted fluxes. Our initial measurements using SMIFTS combined with MODTRAN2 atmospheric modeling have resulted in remotely sensed sea water temperature determination consistent with ground-based measurements, and within the same accuracy ranges. Finally, with further improved technology and use of MODTRAN3 soon to be available, not only will more accurate remotely sensed surface radiances be calculable in this spectral window, but very useful 3-5 μm atmospheric absorption bands such as from carbon and sulfur compounds will be utilizable for purely atmospheric applications.

7. ACKNOWLEDGMENTS

We are grateful to Vern Smiley of NRaD for SMIFTS technical direction, Anu Bowman of Space Application Corp. for coordinating this SMIFTS test flight, to Tim Williams of the University of Hawaii for providing flight support, and to those who provided ground truth data collection: Vern Smiley, David Buck and Bob James also of NRaD, Ed Winter and Donna Winter from TRA, Inc., Ray Maples from SSDC, and John Hinrichs and Anders Daniels from the University of Hawaii. NRaD, TRA, and the University of Hawaii supplied ground truth instrumentation. This work was supported by the Advanced Research Projects Agency AASERT program Contract No. N00014-91-C-0028.

8. REFERENCES

1. Berk, A., L.S. Bernstein, and D.C. Robertson. *MODTRAN: A Moderate Resolution Model for LOWTRAN 7*, 38 p., Air Force Geophysics Laboratory Technical Report AFGL-TR-89-0122, 1989.

2. Blake, P.L. and R.B. Singer. "The removal of atmospheric effects from remotely sensed near-infrared spectral data," *Joint AAS/JRS Symposium, AAS 85-626*, 17 p., 1985.

3. Center for the Study of Active Volcanoes. "Vog and Laze seminar, in abstracts," Hilo, HI, University of Hawaii at Hilo, 26 p., 1991.

4. Gao, Bo-Cai, K.B. Heidebrecht, and A.F.H. Goetz. "Derivation of scaled surface reflectances from AVIRIS data," *Remote Sens. Environ.*, **44**, pp.165,178, 1993.

5. Kahle, A.B., J.P. Schieldge, and R.E. Alley. "Sensitivity of thermal inertia calculations to variations in environmental factors," *Remote Sens. Environ.*,**16**, pp. 211-232, 1984.

6. Kalluri, S.N.V. and R.O. Dubayah . "Comparison of atmospheric correction models for thermal bands of the Advanced Very High Resolution Radiometer over FIFE," *Jour. Geophys. Res.*, **100**, no. D12, pp. 25411-25418, 1995.

7. Kneizys, F.X., E.P. Shettle, W.O. Gallery, J.H. Chetwynd, Jr., L.W. Abreu, J.E.A. Selby, S.A. Clough, and R.W. Fenn. *Atmospheric Transmittance/Radiance: Computer Code LOWTRAN 6*, 200p., Air Force Geophysics Laboratory Technical Report AFGL-TR-83-0187, 1983.

8. Lucey, P.G., T. Williams, K. Horton, K. Hinck, C. Budney, J.B. Raffert, and T.B. Rusk. "SMIFTS: A cryogenically cooled, spatially modulated, imaging Fourier transform spectrometer for remote sensing applications," *Imaging Spectrometry of the Terrestrial Environment*, (G. Vane, ed.), pp. 130-141, 1993.

9. Masuda, K., T. Takashima, and Y. Takayama. "Emissivity of pure and sea waters for the model sea surface in the infrared window regions," *Remote Sens. Environ.*, **24**, pp. 313-329, 1988.

10. McAlister, E.D., W. McLeish, and E.A. Corduan. "Airborne measurements of the total heat flux from the sea during Bomex," *Jour. Geophys. Res.*, **76**, no. 18, pp 4172-4180, 1971.

11. McClain, E.P., W.G. Pichel, and C.C. Walton. "Comparitive performance of AVHRR-based multichannel sea surface temperatures," *Jour. Geophys. Res.*, **90**, no. C6,pp. 11,587-11,601,1985.

12. Press, W.H., S.A. Teukolsky, W.T. Vetterling, and B.P. Flannery. *Numerical Recipes in C*, pp.611, Cambridge University Press, 1992.

13. Ridgway, W.L., R.A. Moose, and A.C. Cogley. *Single and Multiple Scattered Solar Radiation*, 196 p., Air Force Geophysics Laboratory Technical Report AFGL-TR-82-0299 (NTIS No. AD-A126323), 1982.

14. Rinsland, C.P., G.K. Yue, M.R. Gunson, R. Zander, and M.C. Abrams (1994) Mid- infrared extinction by sulfate aerosols from the Mt. Pinatubo eruption. *J. Quant.Spectroscop. Radiat. Transfer.*, **52**, no.3/4, pp. 241-252.

15. Salisbury, J.W. and D.M. D'Aria. "Emissivity of terrestrial materials in the 3-5 μm atmospheric window," *Remote Sensing of the Environment*, **47**, pp. 345-361, 1994.

16. Schluessel, P., H-Y. Shin, W.J. Emery, and H. Grassl. "Comparison of satellite-derived sea surface temperatures with in-situ skin measurements," *Jour. Geophys. Res.*, **92**, pp. 2859-2874, 1987.

17. Smith, F.G. (ed.). *The IR/EO Handbook: Atmospheric Propegation of Radiation*, Vol. 2, pp. 59-63 and 100-109, Environmental Research Institute of Michigan, Ann Arbor, 1993.

18. Sutton, J. and T. Elias. "Volcanic gases create air pollution on the island of Hawaii," U.S. Geological Survey*Earthquakes & Volcanoes*, **24**, pp. 178-196, 1993.

19. Vane, G., R.O. Green, T.G. Chrien, H.T. Enmark, E.G. Hansen, and W.M. Porter. "The Airborne Visible/Infrared Imaging Spectrometer (AVIRIS)," *Remote Sens. Environ.*, **44**, pp.127-143, 1993.

9. FIGURES

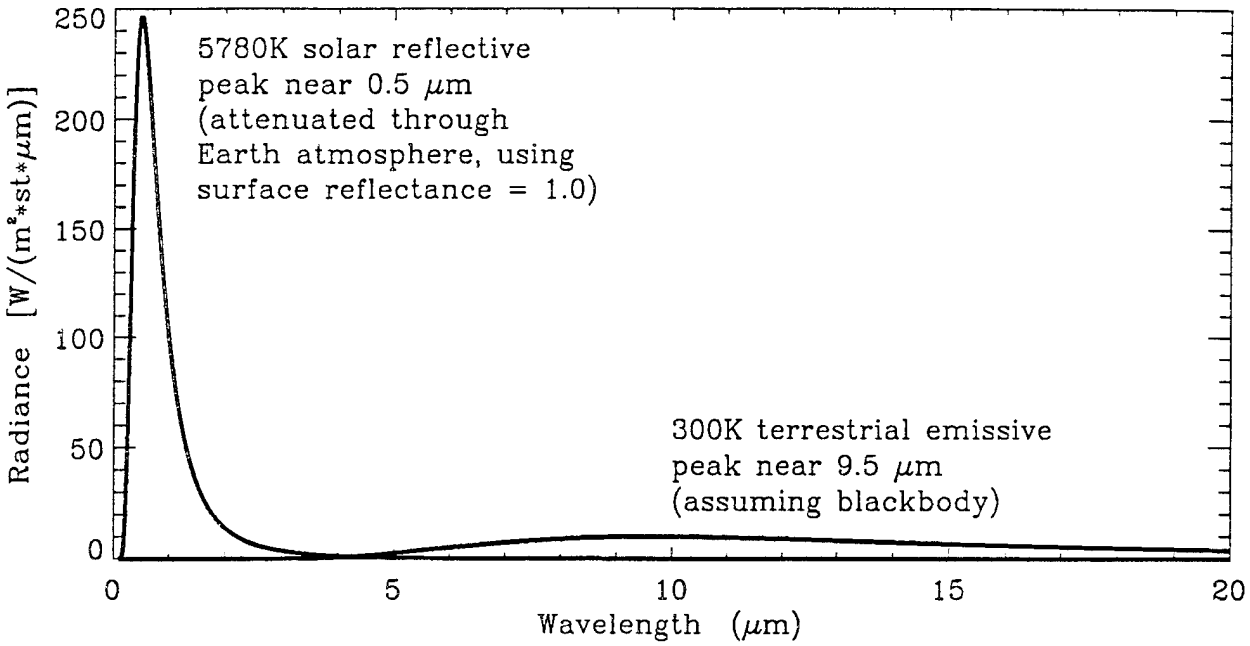

FIGURE 1. Representative terrestrial at-surface radiant fluxes (without specific atmospheric absorption features), showing the relative energy levels of reflection and emission.

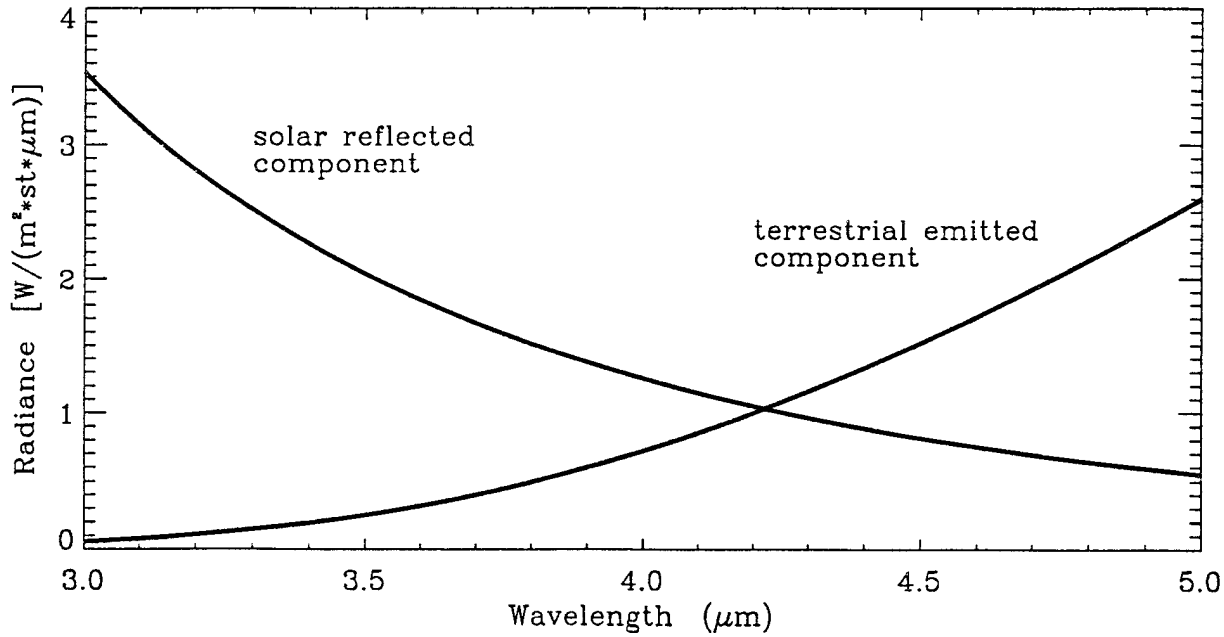

FIGURE 2. Representative terrestrial at-surface radiant fluxes (without specific atmospheric absorption features) in between 3-5 μm, showing the low flux level of both components, as well as their relative equivalence.

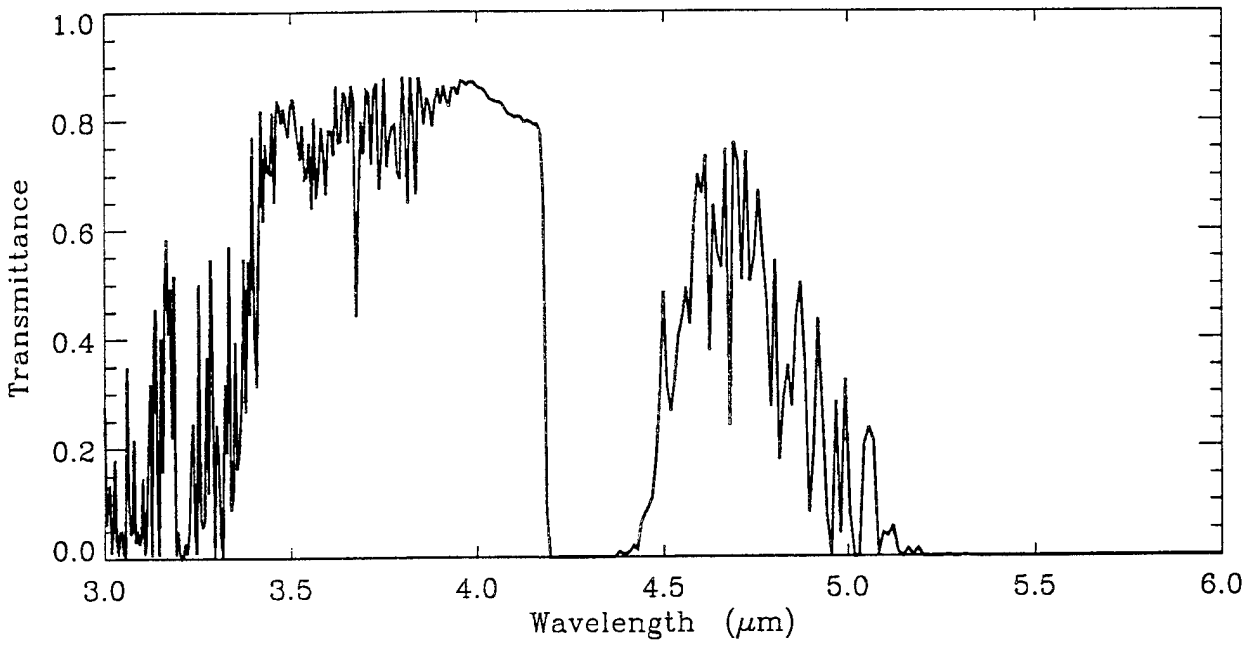

FIGURE 3. MODTRAN2 2 cm^{-1} spectral resolution representation of atmospheric transmittance showing molecular absorptions primarily due to water vapor, gaseous carbon and nitrogen compounds.

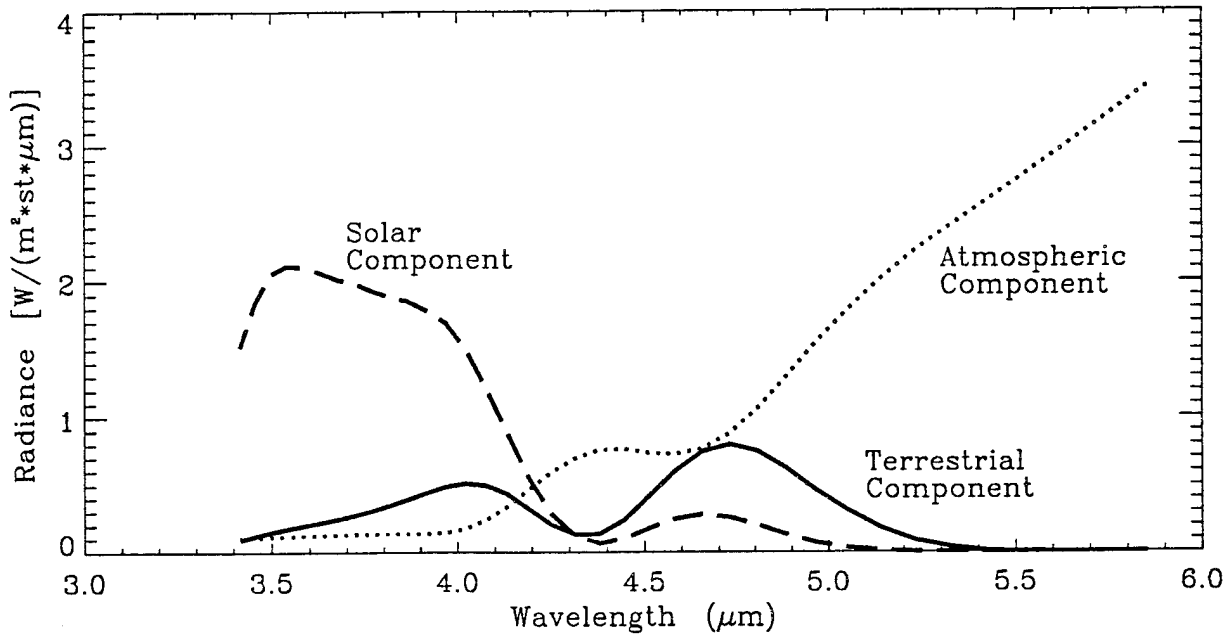

FIGURE 4. Comparison of at-sensor solar reflection (100% albedo surface), terrestrial (blackbody) emission, and atmospheric emission (all at-sensor). Although our surface was seawater (assumed 2.5% albedo), the above illustrates the general equivalence of the three components contributing to the radiance in this wavelength region.

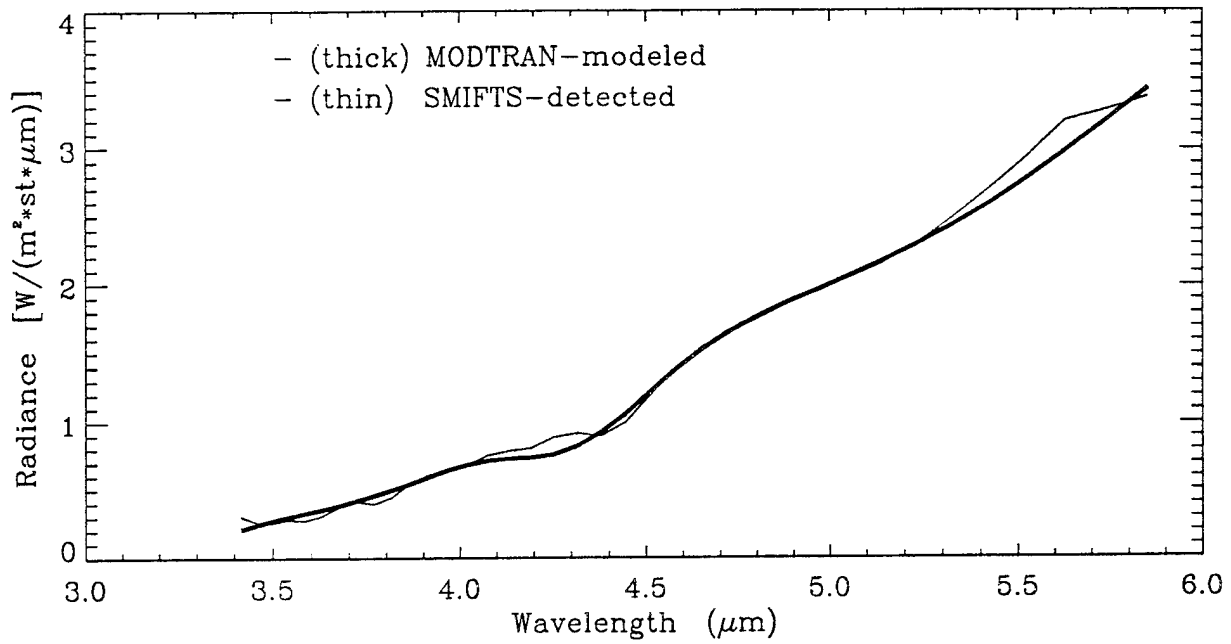

FIGURE 5. MODTRAN-modeled and SMIFTS-detected spectra for 2:30 P.M. May 14, 1994, approximately 2 km over NELHA seawater pond of known surface temperature. The MODTRAN run included the use of concurrent radiosondes, and adjustments to several lower atmospheric layers of radiosonde inputs to account for differences in temperature and relative humidity between NELHA and the radiosonde launch.

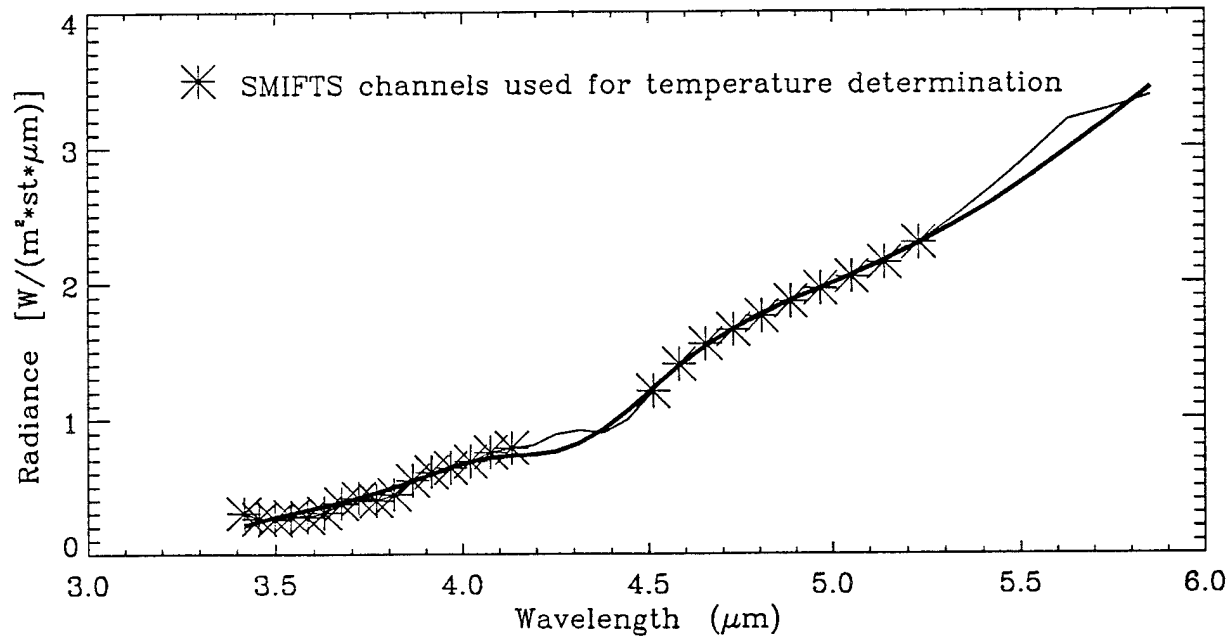

FIGURE 6. Figure 5 repeated to show regions of the modeled and measured spectra where the atmospheric transmittance is not dominated by atmospheric absorptions, used for surface temperature determination.

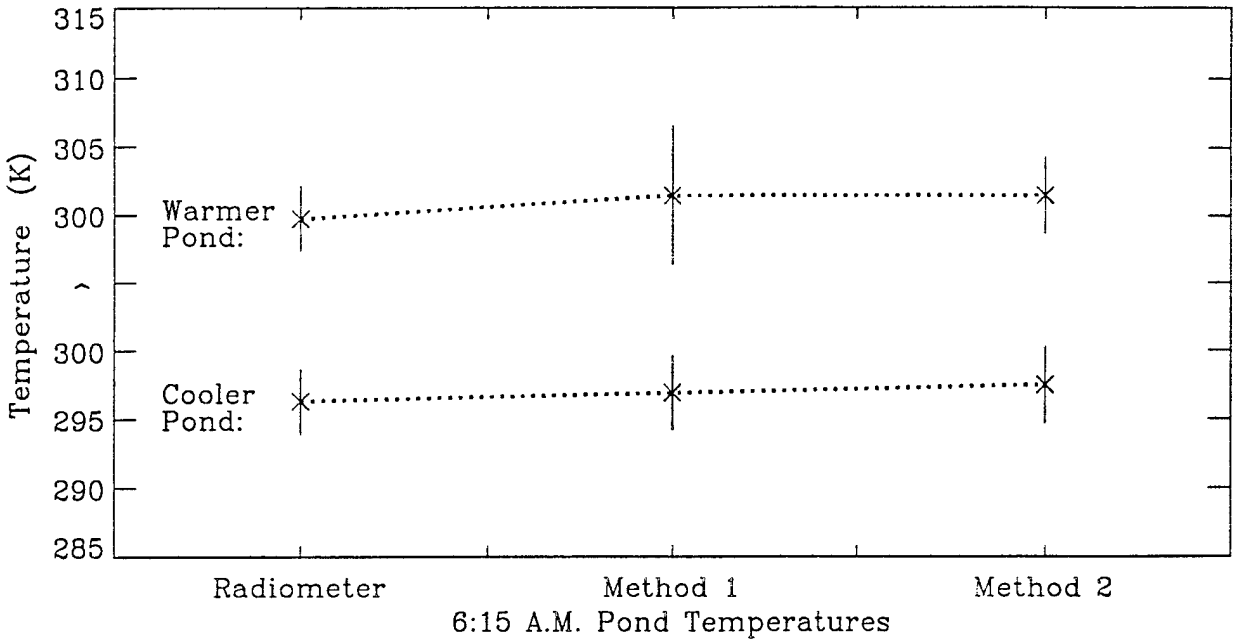

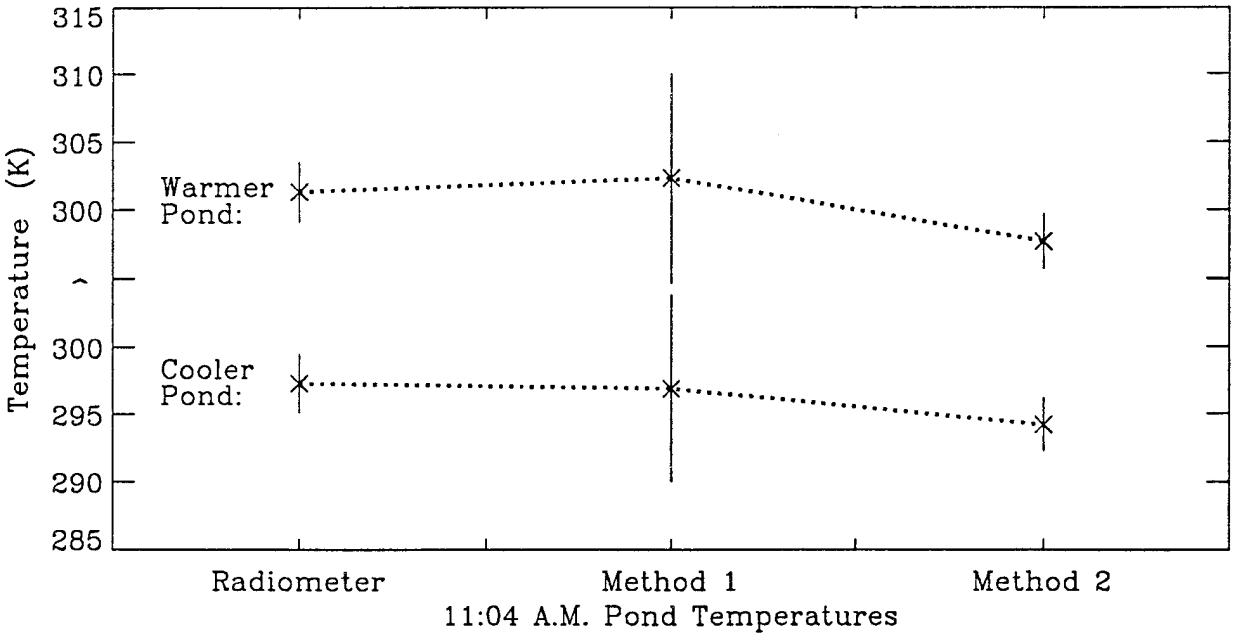

FIGURES 7 & 8. 6:15 A.M. (top) and 11:04 A.M. (bottom) pond temperatures via ground measurement (hand-held radiometer), effective blackbody calculation (method 1), and reverse-MODTRAN modeling (method 2), and the associated root-mean-square errors. Note the y axis scale offset.